Journal of Neurochemistry
Lippincott Williams & Wilkins, Inc., Philadelphia

Induction of Neuronal Apoptosis by Thiol Oxidation: Putative Role of Intracellular Zinc Release

Elias Aizenman, *Amy K. Stout, Karen A. Hartnett, *Kirk E. Dineley, BethAnn McLaughlin, and *Ian J. Reynolds

*Departments of Neurobiology and *Pharmacology, University of Pittsburgh School of Medicine, Pittsburgh, Pennsylvania, U.S.A.*

Abstract: The membrane-permeant oxidizing agent 2,2′-dithiodipyridine (DTDP) can induce Zn^{2+} release from metalloproteins in cell-free systems. Here, we report that brief exposure to DTDP triggers apoptotic cell death in cultured neurons, detected by the presence of both DNA laddering and asymmetric chromatin formation. Neuronal death was blocked by increased extracellular potassium levels, by tetraethylammonium, and by the broad-spectrum cysteine protease inhibitor butoxy-carbonyl-aspartate-fluoromethylketone. *N,N,N′,N′*-Tetrakis-(2-pyridylmethyl)ethylenediamine (TPEN) and other cell-permeant metal chelators also effectively blocked DTDP-induced toxicity in neurons. Cell death, however, was not abolished by the NMDA receptor blocker MK-801, by the intracellular calcium release antagonist dantrolene, or by high concentrations of ryanodine. DTDP generated increases in fluorescence signals in cultured neurons loaded with the zinc-selective dye Newport Green. The fluorescence signals following DTDP treatment also increased in fura-2- and magfura-2-loaded neurons. These responses were completely reversed by TPEN, consistent with a DTDP-mediated increase in intracellular free Zn^{2+} concentrations. Our studies suggest that under conditions of oxidative stress, Zn^{2+} released from intracellular stores may contribute to the initiation of neuronal apoptosis. **Key Words:** Oxidation—Apoptosis—Zinc—Cerebral cortex—Tissue culture.
J. Neurochem. **75,** 1878–1888 (2000).

Zinc has been reported to be toxic to neurons in vitro and in vivo (Choi et al., 1988; Cuajungco and Lees, 1998*a*; Weiss et al., 1993; Koh and Choi, 1994; Manev et al., 1997; Sheline et al., 2000). Heretofore, Zn^{2+}-mediated cell death has been shown to be dependent on influx of the cation into cells because injury could be blocked by cell-impermeant metal chelators (Koh et al., 1996) and by antagonists of voltage- or glutamate-gated ion channels that are permeable to Ca^{2+} (Weiss et al., 1993; Koh and Choi, 1994; Sensi et al., 1997). Zn^{2+} influx has been suggested to contribute to the neuronal damage associated with ischemia and epilepsy as Zn^{2+} is present in synaptic vesicles (Frederickson, 1989), can be released from neurons on depolarization (Assaf and Chung, 1984; Howell et al., 1984; Aniksztejn et al., 1987; Vogt et al., 2000), and translocates from presynaptic sites into postsynaptic neurons (Sloviter, 1985; Koh et al., 1996; Frederickson et al., 1988; Lee et al., 2000).

Rather than existing as a free ion in the cytoplasm, most neuronal Zn^{2+} is packaged either in synaptic vesicles or is tightly complexed to proteins such as metallothionein (MT) and Zn^{2+} finger-containing transcription factors (Frederickson, 1989; Berg, 1990). In the present study we tested the hypothesis that these intracellular stores represent a potential source for Zn^{2+}-mediated neurotoxicity in neurons. As Zn^{2+} can be released from MT in cell-free systems by oxidizing agents that can catalyze disulfide exchange, such as 2,2′-dithiodipyridine (DTDP) (Jiang et al., 1998; Maret and Vallee, 1998), we examined whether a limited exposure of neurons in culture to DTDP resulted in neuronal injury. We also investigated whether the release of Zn^{2+} from intracellular stores following DTDP treatment could be measured with fluorescent probes.

MATERIALS AND METHODS

Cell culture and toxicity assays

Cortical cultures were prepared from embryonic day 16 Sprague–Dawley rats as previously described (Hartnett et al., 1997). In brief, cortices were dissociated and plated onto poly-

Received May 25, 2000; revised manuscript received July 4, 2000; accepted July 5, 2000.

Address correspondence and reprint requests to Dr. E. Aizenman at Department of Neurobiology, University of Pittsburgh School of Medicine, E1456 BST, Pittsburgh, PA 15261, U.S.A. E-mail: redox@pitt.edu

The present address of Dr. A. K. Stout is MitoKor, 11494 Sorrento Valley Road, San Diego, CA 92121, U.S.A.

The present address of Ms. K. A. Hartnett is Beckim Industries, 3625 Watchill Road, Munhall, PA 15120, U.S.A.

Abbreviations used: AM, acetoxymethyl ester; BAF, butoxy-carbonyl-aspartate-fluoromethyl ketone; BAPTA, 1,2-bis(2-aminophenoxy)ethane-*N,N,N′,N′*-tetraacetic acid; $[Ca^{2+}]_i$, intracellular free Ca^{2+} concentration; DTDP, 2,2′-dithiodipyridine; LDH, lactate dehydrogenase; $[Mg^{2+}]_i$, intracellular free Mg^{2+} concentration; MT, metallothionein; TEA, tetraethylammonium; TPEN, *N,N,N′,N′*-tetrakis(2-pyridylmethyl)ethylenediamine; $[Zn^{2+}]_i$, intracellular free Zn^{2+} concentration.

L-lysine-treated tissue culture plates in a growth medium composed of 80% Dulbecco's modified Eagle's medium, 10% Ham's F12-nutrients, and 10% bovine calf serum (heat-inactivated and iron-supplemented) with 25 m*M* HEPES, 24 U/ml penicillin, 24 μg/ml streptomycin, and 2 m*M* L-glutamine. Medium was partially replaced three times a week. Glial cell proliferation was inhibited after 2 weeks in culture with 1–2 μM cytosine arabinoside, at which time the culture medium was reduced to 2% serum without F12-nutrients. At 3–5 weeks in vitro these cultures contain ~10–20% neurons (Rosenberg and Aizenman, 1989; Rosenberg, 1991). Toxicity assays were performed on 4-week-old cultures (25–29 days in vitro). Immediately before drug treatment, the cells were rinsed (200:1) in minimum essential medium with Earle's salts containing 0.01% bovine serum albumin and 25 m*M* HEPES. Cells were exposed to DTDP for 10 min at 37°C in 5% CO_2. Treatment was removed by serial dilution (200:1), and the cells were returned to the incubator.

Neuronal viability was determined 18–20 h following exposure using a lactate dehydrogenase (LDH)-based in vitro toxicology assay kit (Sigma, St. Louis, MO, U.S.A.). Medium samples (40 μl) were analyzed spectrophotometrically (at 490 and 630 nm) according to the manufacturer's protocol, to obtain a measure of cytoplasmic LDH release from dead and dying neurons. Toxicity was assessed as the ratio of LDH_{DTDP} / $LDH_{Vehicle}$. LDH activity can be measured from neurons undergoing apoptosis because phagocytosis of dead cells does not take place in our culture system. Relative neuroprotection provided by the various agents tested was expressed as neuronal protection, which was derived by the following equation: $100 - \{[(LDH_{DTDP+treatment} / LDH_{Vehicle+treatment}) / (LDH_{DTDP} / LDH_{Vehicle})] \times 100\}$.

Forebrain neuronal-enriched cultures were prepared from embryonic day 17 rat fetuses as previously described (McLaughlin et al., 1998). Dissociated cells were plated on poly-L-ornithine-treated tissue culture plates in a growth medium composed of 80% Dulbecco's modified Eagle's medium (high glucose with L-glutamine and without sodium pyruvate; GibcoBRL, Grand Island, NY, U.S.A.), 10% Ham's F12-nutrients, 10% bovine calf serum (heat-inactivated), and 1× antimycotic/antibiotic mixture (with amphotericin B and streptomycin sulfate; GibcoBRL). Cultures were maintained in an incubator at 37°C in 5% CO_2. Glial cell proliferation was inhibited after 48 h in culture with 1–2 μM cytosine arabinoside. After 3 days in vitro, the serum-containing medium was replaced with a serum-free solution comprised of Neurobasal medium (without L-glutamine; GibcoBRL), 1× B27 supplement (GibcoBRL), and 1× antimycotic/antibiotic mixture. Toxicity assays on neuron-enriched cultures were performed in tissue culture plates containing plastic grid coverslips at 6–8 days following dissociation. Cells were rinsed (200:1) with HEPES-buffered salt solution before a 10-min exposure to 10 μM DTDP. Treatment was terminated first by rinsing (200:1) and then by adding serum-free Neurobasal medium (containing 1× antimycotic/antibiotic mixture but without the B27 supplement) to the cultures. Cultures were maintained overnight at 37°C in 5% CO_2. Viability was determined 18–20 h following exposure using trypan blue exclusion staining and viability counts. Cells were counted (three to five areas of the labeled plastic grid) both before and following treatment by a person blinded to the arrangement of the treatment groups. Counts are expressed as percentages of the pre-exposure counts obtained from the same grid areas.

To determine the extent of asymmetric chromatin condensation induced by DTDP, Hoechst 33342 staining was performed on neuron-enriched cultures. Toxicity assays were performed in tissue culture plates containing glass coverslips. Hoechst staining was performed 18–20 h following DTDP exposure. Cultures were washed briefly in phosphate-buffered saline, fixed in 10% formaldehyde for 10 min, and incubated in 5 μg/ml Hoechst 33342 dye (Sigma) for an additional 10 min. Cultures were washed twice with phosphate-buffered saline, and the coverslips were mounted onto slides using Mowoil mounting medium. Fluorescence was visualized using a Nikon Eclipse E600 microscope with a fluorescent light source and bright-field illumination, and the percentage of apoptotic nuclei from three to five fields per coverslip was calculated by a person blinded to the treatment conditions.

Induction of DNA laddering by DTDP in cortical neurons was evaluated as described by McLaughlin et al. (1998). In brief, cells previously exposed to DTDP were scraped from their dishes in a lysis solution (0.1 *M* sodium EDTA, 1% sodium dodecyl sulfate, 200 m*M* Tris, and 0.5 mg of proteinase K). Proteins were removed by centrifugation, and DNA was precipitated with 100% ethanol. DNA samples were electrophoresed on a 1.8% agarose gel, which was later stained with ethidium bromide.

Fluorescence imaging

Changes in intracellular free Zn^{2+} concentration ($[Zn^{2+}]_i$) in cultured neurons were monitored with the zinc-selective fluorescent indicator Newport Green. In addition, previous studies in this and other laboratories have demonstrated the usefulness of the fluorescent indicators magfura-5, magfura-2, fura-2, and fluo-3 for measurement of $[Zn^{2+}]_i$ under conditions in which the intracellular free Ca^{2+} concentration ($[Ca^{2+}]_i$) does not change (Sensi et al., 1997; Cheng and Reynolds, 1998). $[Zn^{2+}]_i$ was measured using methods and equipment previously described for measuring increases in $[Ca^{2+}]_i$ (Stout and Reynolds, 1999). In brief, neurons were loaded with dye via incubation in HEPES-buffered salt solution containing 5 μM Newport Green acetoxymethyl ester (AM), magfura-2 AM, fura-2 AM, or fluo-3 AM, 5 mg/ml bovine serum albumin, and 0.5% dimethyl sulfoxide at 37°C for ~30 min. Following loading, coverslips were rinsed with HEPES-buffered salt solution, mounted in a recording chamber, and perfused with HEPES-buffered salt solution at a rate of 20 ml/min. All recordings were made at room temperature (20–25°C). Background fluorescence values (determined from cell-free regions of each coverslip) were subtracted from all signals. The imaging system used in these studies consisted of a Nikon Diaphot 300 microscope fitted with a 40× quartz objective, a Dage-MTI cooled-CCD camera with 640- × 480-pixel resolution in combination with a Dage-MTI Gen II Sys image intensifier, a software package from Compix (Cranberry, PA, U.S.A.), and a 75-W xenon lamp-based monochromator light source from Applied Scientific Instrumentation (Eugene, OR, U.S.A.). Cells were alternately illuminated with 335 and 375 nm light for magfura-2 measurements or with 345 and 375 nm light for fura-2 measurements. Newport Green and fluo-3 were illuminated at 490 or 504 nm, respectively. Attenuation of incident light was achieved with neutral density filters (ND 2 for 1% transmittance; Omega Optical, Brattleboro, VT, U.S.A.). Emitted light passed through a 515 nm dichroic mirror and a 535 ± 12.5 nm band pass filter (Omega Optical). Simultaneous measurements were performed in 16–32 neurons per coverslip.

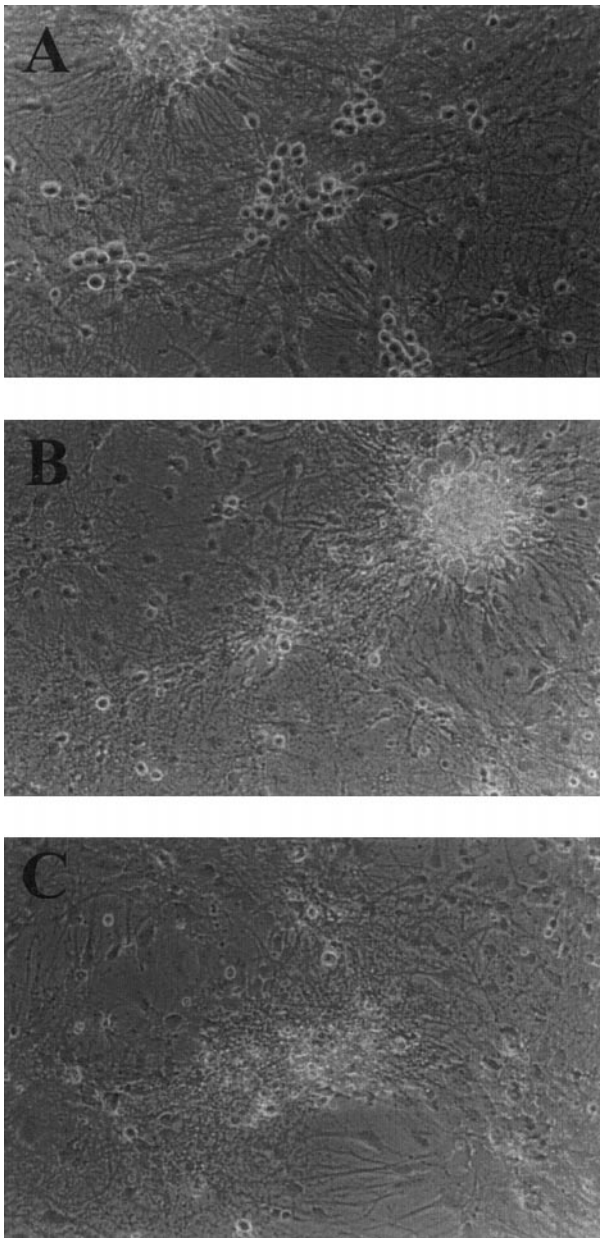

FIG. 1. Neurotoxicity of DTDP. Mixed cultures of neurons and glia were exposed to (**A**) vehicle (minimum essential medium with 0.01% bovine serum albumin and 25 m*M* HEPES, 10 min), (**B**) DTDP (100 μM, 10 min), or (**C**) NMDA (100 μM, 30 min) and photographed 24 h later. Phase-bright neurons appear on top of a glial cell layer. Note the similar pattern of toxicity elicited by DTDP and NMDA.

RESULTS

DTDP is neurotoxic to neurons in culture

Mixed cortical cultures exposed for 10 min to 100 μM DTDP underwent widespread neuronal cell death within 24 h. This toxicity appeared to spare the underlying glial cell layer, a phenomenon that is commonly observed when cells are exposed to NMDA (Fig. 1). Exposure to increasing concentrations of DTDP (10 min) caused the release of LDH from the cultures in a dose-dependent fashion (Fig. 2). Sister cultures that had been previously exposed to 1 m*M* kainate overnight to remove the neuronal component of the cultures also showed a dose-dependent increase in LDH release on DTDP exposure, suggesting that high doses of this agent could promote gliotoxicity. However, this LDH release was much less pronounced that that observed in the presence of neurons (Fig. 2), even though glia constitute ~80–90% of the cellular mass in this preparation (Rosenberg and Aizenman, 1989; Rosenberg, 1991). This argues that neurons are, in fact, appreciably more sensitive than glial cells to the toxic actions of DTDP.

To begin to determine the mechanism of DTDP-induced cell death, we evaluated cultures for hallmark features of apoptosis. First, we extracted DNA from DTDP (100 μM)-treated cultures at various time points to look for the presence of DNA laddering and noted that internucleosomal fragmentation was present 6 h after exposure to the toxin (Fig. 3A). Second, we observed that the broad-spectrum cysteine protease inhibitor butoxy-carbonyl-aspartate-fluoromethyl ketone (BAF; 100 μM) substantially abrogated DTDP toxicity (Fig. 3B). Third, we found that DTDP toxicity was significantly inhibited when high extracellular KCl (25 m*M*) was present during the DTDP exposure (Fig. 3B). These elevated K^+ conditions have previously been shown to block staurosporine-induced apoptosis in cultured neurons by blocking K^+ efflux through tetraethylammonium (TEA)-sensitive channels (Yu et al., 1997). Indeed, we found that 10 m*M* TEA effectively inhibited DTDP toxicity in our cultures (Fig. 3B). Finally, asymmetric chromatin formations were observed following Hoechst staining in neuron-enriched cultures treated for 10 min with 100 μM DTDP (Fig. 4). Given that our neuron-enriched cultures contain <0.5% nonneuronal elements,

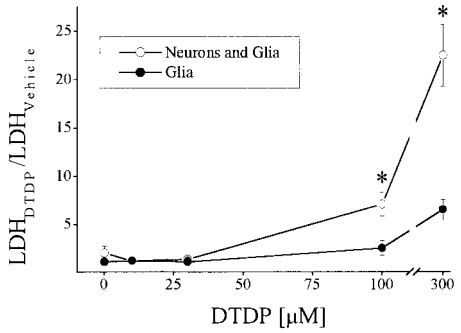

FIG. 2. DTDP kills neurons preferentially over glia. Mixed neuronal and glial cortical cultures were first exposed to minimum essential medium alone or in the presence of 1 m*M* kainate overnight to kill neurons and generate glial cultures. Both cultures were then subsequently exposed to increasing concentrations of DTDP for 10 min. After 18–20 h, LDH release was measured. Results for cell toxicity ($LDH_{DTDP}/LDH_{Vehicle}$) are expressed as mean ± SEM (bars) values of four to seven experiments performed in quadruplicate. *$p < 0.05$ by unpaired two-tailed *t* test, indicating toxicity was significantly different between mixed and glial cultures.

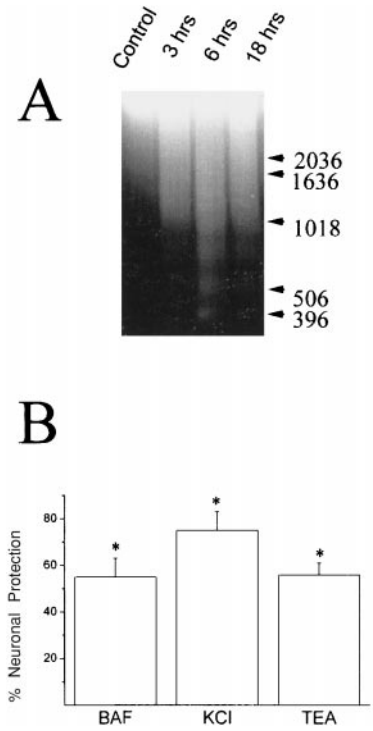

FIG. 3. DTDP induces neuronal apoptosis. **A:** Induction of DNA laddering in cortical cultures by DTDP (100 μM, 10 min). DNA was obtained from control cells and from DTDP-treated cultures at 3, 6, and 18 h following exposure. Note that the lane from control cultures has a high-molecular-weight band representative of intact DNA with no laddering. DNA laddering is observed in DTDP-treated cultures after 6 h. **B:** Inhibition of DTDP neurotoxicity suggests cell death is apoptotic. Mixed cortical cultures were exposed to DTDP (100 μM, 10 min) in the presence or absence of 100 μM BAF, 25 mM KCl, or 10 mM TEA. After 18–20 h, LDH release was measured. Data are mean ± SEM (bars) values for neuroprotection (see text) from experiments performed four to six times in quadruplicate. $^*p < 0.001$ by one-sample two-tailed t test, indicating significant neuroprotection.

this observation proved that the apoptotic phenotype following DTDP treatment was present in neurons. We also observed that DTDP-induced chromatin condensation was virtually abolished by 100 μM BAF (Fig. 4D). The percentage of apoptotic nuclei present in these cultures was reduced from 38 ± 7% in the DTDP-treated cultures to 5 ± 4% in cultures treated with DTDP and 100 μM BAF (n = 4; $p < 0.01$ by unpaired t test). In addition, total cell viability was significantly restored in these cultures when 100 μM BAF was included during DTDP exposure (Fig. 5).

DTDP has previously been used to oxidize and activate ryanodine receptors to release Ca^{2+} from intracellular pools (Eager et al., 1997). We thus evaluated whether DTDP toxicity was due to intracellular calcium release or, indirectly, by inducing glutamate release and producing excitotoxicity. Mixed cortical cultures were exposed to DTDP (100 μM, 10 min) in the presence or absence of 50 μM ryanodine, 20 μM dantrolene (to block ryanodine receptors), or 10 μM MK-801 (to block NMDA receptor activation). After 18–20 h, LDH release was measured. No neuroprotection was observed with any of these agents (data not shown).

DTDP releases Zn^{2+} from intracellular stores

Having ruled out intracellular Ca^{2+} release and excitotoxicity as contributors to DTDP toxicity, we next assessed the possibility that the thiol oxidant may be causing Zn^{2+} release from intracellular stores as suggested by prior cell-free studies (Jiang et al., 1998; Maret and Vallee, 1998). To monitor increases in $[Zn^{2+}]_i$ we used a series of fluorescent indicators (Canzoniero et al., 1997; Cheng and Reynolds, 1998; Sensi et al., 1999). Exposure of neurons loaded with the Zn^{2+}-selective dye Newport Green to 100 μM DTDP resulted in a slow increase in the fluorescence signal (4.66 ± 0.39 arbitrary fluorescence units, or 12.8%; n = 43) consistent with an increase in $[Zn^{2+}]_i$. This increase could be rapidly reversed by addition of 25 μM *N,N,N′,N′*-tetrakis(2-pyridylmethyl)ethylenediamine (TPEN) (Fig. 6A). A similar effect was observed when neurons were loaded with magfura-2 (Fig. 6B), which we have previously used to monitor $[Zn^{2+}]_i$ (Cheng and Reynolds, 1998). It is interesting that the increase in magfura-2 ratio was observed in cells bathed in Zn^{2+}-free conditions and previously treated with TPEN, thus suggesting that the DTDP-sensitive pool is not extracellular, nor is it readily chelatable before oxidant treatment. The Zn^{2+}-free solution contained 1 mM Ca^{2+}-saturated disodium EDTA to chelate Zn^{2+}. The $-\log K_D$ of calcium for EDTA is 10.73, whereas the $-\log K_D$ for zinc is 16.8 (MiniSCD Database, version 4; Academic Software, Otley, U.K.).

We performed several additional experiments to investigate further the identity of the ion mobilized by DTDP. By exploiting the high affinity of Zn^{2+} binding to fura-2, magfura-2, and fluo-3, the possibility that dye changes are due to alterations in $[Ca^{2+}]_i$ or another intracellular cation can be addressed. DTDP exposure (100 μM, 10 min) caused an increase in the fluorescence ratio in primary cultures of rat forebrain neurons previously loaded with fura-2 AM (Fig. 7A). The mean ± SEM increase in the fura-2 ratio on DTDP stimulation was 0.21 ± 0.005 over baseline, which was 0.73 ± 0.002 (n = 293). This DTDP-induced increase in the fura-2 signal was relatively small compared with the mean Ca^{2+}-mediated increase in the fura-2 ratio obtained in these cells on stimulation with 100 μM NMDA plus 10 μM glycine for 15 s (1.78 ± 0.030; Fig. 7B). Similar to what we described above, DTDP also caused an increase in the fluorescence ratio in neurons loaded with magfura-2 AM (Fig. 7C). The mean ± SEM increase in the magfura-2 ratio on DTDP stimulation (100 μM, 10 min) was 0.046 ± 0.001 over baseline (0.30 ± 0.001, n = 86). This signal is comparable to that observed following addition of <1 μM extracellular zinc in the presence of pyrithione (Dineley et al., 2000). For comparison, the mean ± SEM increase in the magfura-2 ratio obtained in these cells on stimulation with 100 μM NMDA plus 10 μM glycine for 1 min was 0.23 ± 0.023. DTDP also

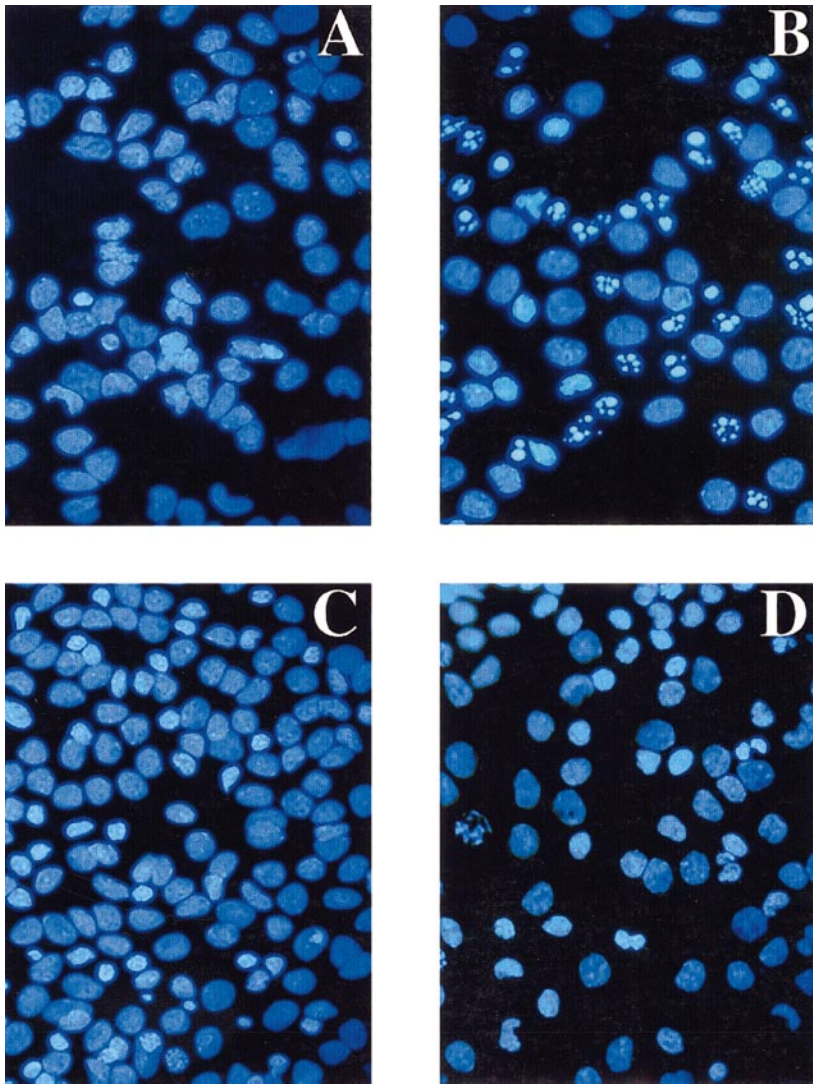

FIG. 4. DTDP-induced caspase-dependent asymmetric chromatin condensation in neurons. Neuron-enriched cultures were exposed to (**A**) vehicle, (**B**) DTDP (10 μM, 10 min), (**C**) BAF (100 μM), or (**D**) DTDP plus BAF. Cultures were fixed at 18–20 h, stained with Hoechst 33342 (5 μg/ml), and visualized with a microscope equipped with a fluorescent light source.

increased the fluorescence signal in fluo-3-loaded neurons (data not shown). DTDP stimulation increased the fluo-3 signal to 2.4 ± 0.05 times the basal level, whereas stimulation with 100 μM NMDA plus 10 μM glycine caused a 7.6 ± 0.2-fold increase in the fluo-3 signal (n = 115; data not shown).

Although three of the four dyes used are typically used to measure increases in $[Ca^{2+}]_i$, the DTDP-induced signal changes reported here likely represent increases in $[Zn^{2+}]_i$. This is supported by three lines of evidence. First, Newport Green shows little or no change in signal in response to increases in $[Ca^{2+}]_i$ or intracellular free Mg^{2+} concentration ($[Mg^{2+}]_i$) (data not shown). Second, increases in $[Ca^{2+}]_i$ of a magnitude sufficient to cause changes in the magfura-2 ratio (K_D for Ca^{2+} of ~25 μM) would cause very large, possibly saturating, responses when measured with the high-affinity indicators fura-2 and fluo-3 [K_D values for Ca^{2+} of 145 and 390 nM, respectively (Stout and Reynolds, 1999)]. Third, the three Ca^{2+}-sensitive dyes undergo fluorescence changes

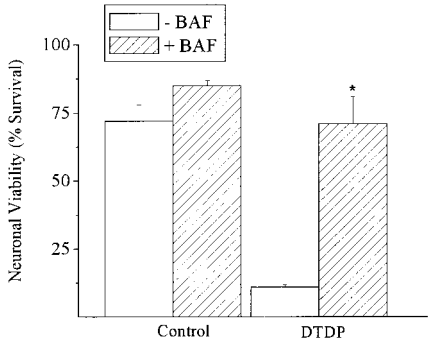

FIG. 5. DTDP toxicity is abolished by BAF in neuronal cultures. Neuron-enriched cultures were exposed to vehicle, BAF (100 μM), DTDP (10 μM, 10 min), or DTDP plus BAF. Viable cells were counted before the treatments and 18–20 h later. Data are mean ± SEM (bars) values from three experiments. *$p < 0.05$ by paired t test, indicating viability is significantly greater in the DTDP + BAF group versus DTDP alone.

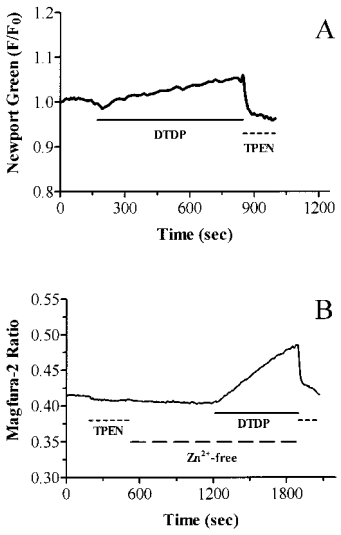

FIG. 6. DTDP causes increases in $[Zn^{2+}]_i$ in neurons. **A:** Neurons loaded with the Zn^{2+}-specific fluorophore Newport Green were exposed to DTDP (100 μM, 10 min; dashed line). DTDP responses were reversed by treatment with TPEN (25 μM, 2.5 min; solid line). The trace depicts the mean change in fluorescence (F/F_0) observed in a field of neurons from a single coverslip and is representative of three separate experiments. DTDP-treated neurons exhibited an increase in Newport Green fluorescence (arbitrary units) of 4.66 ± 0.39 (n = 43), which constituted an average increase of ~12.8%. **B:** DTDP releases Zn^{2+} from tightly bound intracellular stores. Neurons loaded with magfura-2 were exposed to TPEN (25 μM, 5 min; solid line) and subsequently washed with Zn^{2+}-free buffer (large dashed line). After 10 min, DTDP (100 μM; dashed line) was added to the Zn^{2+}-free perfusate for an additional 10 min. The experiment was terminated with application of TPEN (25 μM, 2.5 min; solid line). The trace depicts the mean ratio change observed in a single field of cells and is representative of three separate experiments. Neurons subjected to this series of treatments showed an average magfura-2 ratio increase of 0.072 ± 0.005 units (n = 32).

on Zn^{2+} binding, and the affinities of fura-2, fluo-3, and magfura-2 for Zn^{2+} are similar (low nanomolar K_D values) (Grynkiewicz et al., 1985; Simons, 1993), whereas their affinities for Ca^{2+} and Mg^{2+} vary considerably. Hence, all three dyes detect increases in $[Zn^{2+}]_i$ in the same concentration range. Fourth, the increases in the fluorescence signals observed with magfura-2, fura-2, and fluo-3 were completely reversed by perfusion with TPEN (25 μM; Fig. 7C and D and data not shown). TPEN has a high affinity for Zn^{2+} (K_D = 0.26 fM) but has an affinity for Ca^{2+} that is lower than that of any of the dyes used here [K_D = 40 μM (Arslan et al., 1985)]. Therefore, if the DTDP-induced responses did reflect increases in $[Ca^{2+}]_i$, it is unlikely that TPEN could bind free Ca^{2+} sufficiently to reverse the response. It is also unlikely that these DTDP responses represent increases in $[Mg^{2+}]_i$ because neither fura-2 nor fluo-3 responds to increases in $[Mg^{2+}]_i$ (Stout and Reynolds, 1999) and because the affinity of TPEN for Mg^{2+} [K_D = 20 mM (Arslan et al., 1985)] would not be sufficient to compete with magfura-2 in chelating Mg^{2+} and reversing the response (K_D for Mg^{2+} of 1.9 mM). Thus, both the relative magnitude of the responses measured with the different dyes and the reversibility with TPEN are consistent with the DTDP-induced responses being due to increases in $[Zn^{2+}]_i$.

Previous experiments by our group have demonstrated increases in $[Zn^{2+}]_i$ in the 40–100 nM range on exposure to Zn^{2+} under conditions in which $[Ca^{2+}]_i$ and $[Mg^{2+}]_i$ do not change (Cheng and Reynolds, 1998). When we used this previous Zn^{2+} stimulation paradigm with the imaging system used in the present study, we observed responses similar in magnitude to those induced by DTDP, suggesting DTDP responses are also in the nanomolar range. As DTDP has previously been reported to oxidize and activate ryanodine receptors to release Ca^{2+} from intracellular pools (Eager et al., 1997), our results suggest that intracellular ion changes associated with this reagent might be reevaluated to determine if the observed responses represented increases in $[Zn^{2+}]_i$ instead of $[Ca^{2+}]_i$. The reversal with TPEN observed here could also be consistent with DTDP-induced increases in the intracellular free Cu^{2+} concentration, but the fact that Newport Green does not respond to copper makes this possibility unlikely. Finally, both Fe^{2+} and Fe^{3+} produce a concentration-dependent quenching of fura-2 and magfura-2 in vitro (data not shown). Thus, it is also highly unlikely that the fluorescent changes observed in this study represent alterations in intracellular free iron levels.

As further evidence that the neuronal DTDP responses were mediated by increases in $[Zn^{2+}]_i$ and not $[Ca^{2+}]_i$, we showed that the DTDP-induced increases in the fura-2 signal were completely blocked when cells were loaded with a low concentration of 1,2-bis(2-aminophenoxy)ethane-*N*,*N*,*N*′,*N*′-tetraacetic acid (BAPTA) AM before DTDP exposure (10 μM for 10 min; Fig. 7D). Although BAPTA can chelate both Zn^{2+} and Ca^{2+}, it has a higher affinity for Zn^{2+} (Csermely et al., 1989), and BAPTA had only a minor effect on the NMDA-stimulated increases in $[Ca^{2+}]_i$ in these cells at the concentration used here (Fig. 7D). DTDP-induced increases in the fura-2, magfura-2, and fluo-3 responses were also reversed by the sulfhydryl reducing agent dithiothreitol (Fig. 7A and data not shown). Reversal with dithiothreitol is also consistent with the responses being due to increases in $[Zn^{2+}]_i$ because this agent can act as a Zn^{2+} chelator (Cornell and Crivaro, 1972) and could also act to reduce MT back to the form that has high affinity for Zn^{2+} (Jiang et al., 1998; Maret and Vallee, 1998).

Low concentrations of a zinc chelator abolishes DTDP neurotoxicity

Given that our fluorescent dye experiments indicated that zinc released from an oxidation-sensitive store was observed following DTDP exposure, we next evaluated the contribution of this free Zn^{2+} to DTDP-induced apoptosis. We found that DTDP toxicity in neuron-enriched cultures was substantially inhibited by very low concentrations of TPEN (10 nM). The use of low concentrations of TPEN for a very limited exposure time

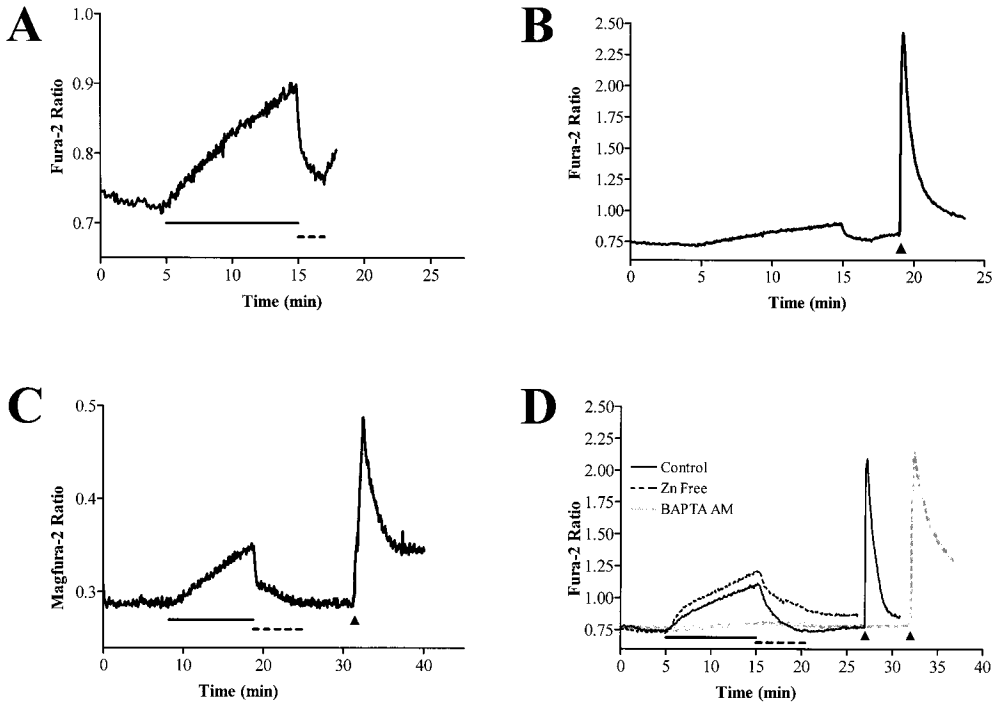

FIG. 7. Further characterization of DTDP-induced zinc release. **A:** Neurons loaded with the fluorescent indicator fura-2 AM were exposed to DTDP (100 μM, 10 min; solid line). DTDP responses were reversed by exposure to dithiothreitol (5 m*M*, 2 min; dashed line). **B:** For comparison, the responses obtained on stimulation with NMDA + glycine (100 μM + 10 μM, 15 s, arrowhead) in the same fura-2-loaded neurons are shown. **C:** Neurons loaded with the fluorescent indicator magfura-2 AM were exposed to DTDP (100 μM, 10 min; solid line). DTDP responses were reversed by exposure to TPEN (25 μM, 6 min). For comparison, the responses obtained on stimulation with NMDA + glycine (100 μM + 10 μM, 1 min, arrowhead) are also shown. **D:** Neurons loaded with the fluorescent indicator fura-2 AM were exposed to DTDP (100 μM, 10 min; solid line). Zn^{2+}-free buffer was present during DTDP stimulation as indicated. Cells were preloaded with BAPTA AM (10 μM, 10 min) as indicated. DTDP responses were reversed by exposure to TPEN (25 μM, 6 min; dashed line). For comparison, the responses obtained on stimulation with NMDA + glycine (100 μM + 10 μM, 15 s, arrowheads) in the same fura-2-loaded neurons are also shown. Each trace represents the mean results from a field of 16–32 neurons from separate coverslips. Similar results were obtained with two to 14 additional coverslips for each condition.

avoided any potential neurotoxic actions of the chelating agent itself, which have been reported by other investigators using very high concentrations of this substance (Ahn et al., 1998; Adler et al., 1999; Virag and Szabo, 1999; although see Shumaker et al., 1998). These neuroprotective actions of TPEN were detected both by Hoechst staining and by cell counting (Fig. 8). In addition, two other metal chelators, BAPTA AM (3 μM) and magfura-2 AM (5 μM) also induced significant neuroprotection against a 100 μM DTDP exposure (BAPTA, 35.0 ± 13.4% neuroprotection, n = 7; magfura-2, 57.8 ± 1.2%, n = 3; $p < 0.05$ and $p < 0.001$, respectively, by two-tailed one-sample *t* test). Although it is conceivable that all these metal chelators block DTDP toxicity by other mechanisms, such as preventing DTDP from inducing Zn^{2+} release from MT, we believe that the simplest explanation to account for these findings is that the chelating agents quickly scavenge any Zn^{2+} released by DTDP. The fact that nanomolar concentrations of TPEN were protective in these studies further supports our contention that DTDP toxicity is due to Zn^{2+} and not Ca^{2+} because the low concentration of TPEN used would not be effective at buffering even resting $[Ca^{2+}]_i$ in these cells.

DISCUSSION

Prior studies have found that elevated $[Zn^{2+}]_i$ may be toxic to neurons following transport into cells via various entry routes (Choi et al., 1988; Weiss et al., 1993; Koh and Choi, 1994; Manev et al., 1997; Sensi et al., 1997; Cuajungco and Lees, 1998*a*). Recent reports by Vallee and colleagues suggest that Zn^{2+} binding and release inside the cell are dynamic processes that are intrinsically linked to the redox status of cell (Jacob et al., 1998; Jiang et al., 1998). The results presented in this study suggest that Zn^{2+} released from such intracellular stores may contribute to neuronal injury under conditions of oxidative stress. These studies thus provide evidence for a previously unrecognized link between oxidative stress and neuronal apoptosis. Furthermore, because there is a substantial body of evidence that links oxidative stress to chronic neurodegenerative disease states, our findings suggest that neuronal injury following intracellular release of Zn^{2+} may be of considerable significance. Given the ubiquitous expression of MT and the fact that zinc is the second most abundant transition metal in the CNS, metalloprotein-bound zinc could be an important component of neurodegeneration throughout the brain. The

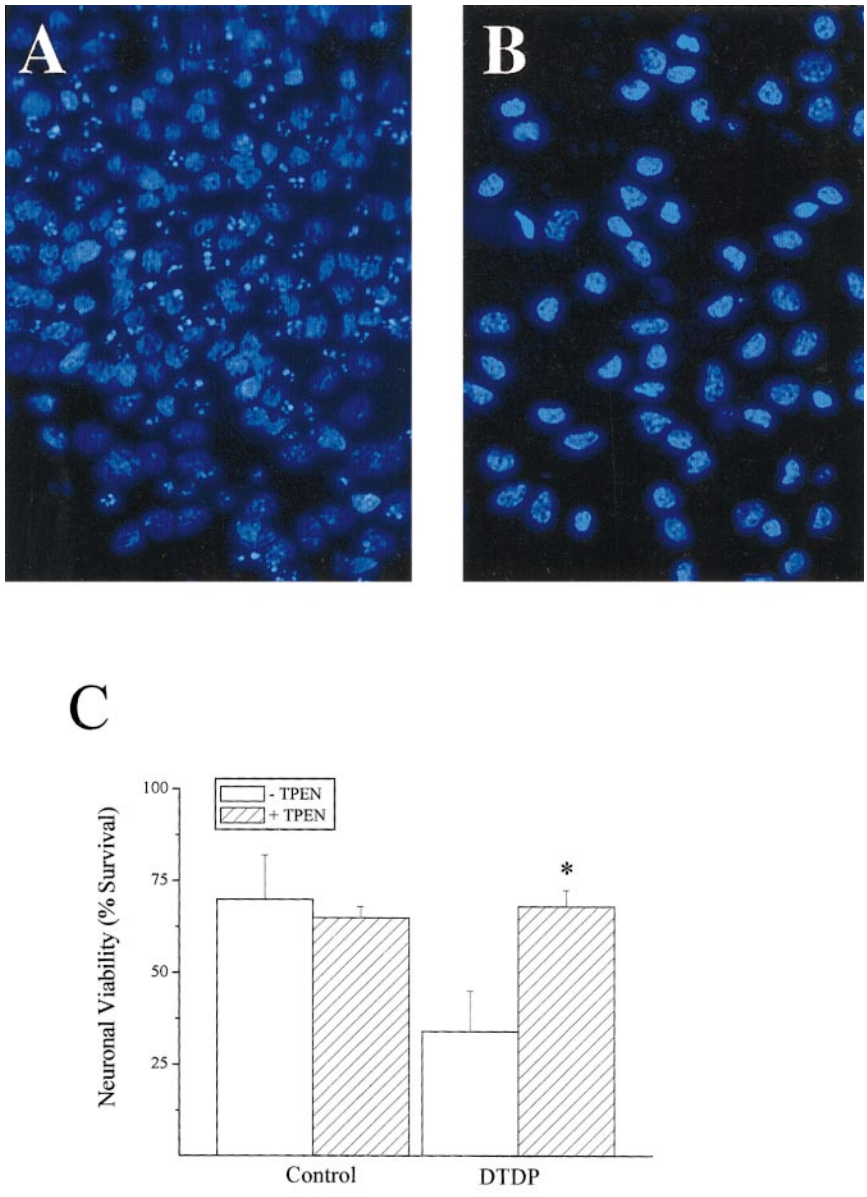

FIG. 8. Low concentrations of a zinc chelator are neuroprotective against DTDP. Neuron-enriched cultures were exposed to vehicle or DTDP (10 μM, 10 min) in the (**A**) absence or (**B**) presence of 10 n*M* TPEN. Cultures were fixed at 18–20 h, stained with Hoechst 33342 (5 μg/ml), and visualized with a microscope equipped with a fluorescent light source. **C:** Neuron-enriched cultures were exposed to vehicle or DTDP (10 μM, 10 min) in the presence or absence of TPEN (10 n*M*). Viable cells were counted before treatments and 18–20 h later to calculate neuronal viability. Data are mean ± SEM (bars) values from three experiments. $^*p < 0.05$ by paired *t* test, indicating viability is significantly greater in the DTDP + TPEN group versus DTDP alone.

use of DTDP thus provides a means to induce zinc release from a physiologically relevant and highly toxic pool.

We recognize that in our present studies we have used an oxidizing agent that, although well characterized for its effects on releasing zinc from MT (Jiang et al., 1998; Maret and Vallee, 1998), is hardly a relevant pathophysiological oxidation stimulus. Nonetheless, many endogenous oxidants are well known for their ability to cross-link or modify disulfide bonds and modify protein function (Aizenman et al., 1990). Therefore, the cell death pathway we describe here may have far-reaching implications in neuronal injury. Oxidative stress has been shown to induce rapidly MT gene expression following the activation of a metal response promoter that is selective for zinc [metal-responsive transcription factor (Dalton et al., 1996; Andrews, 1999)], providing indirect evidence that oxidative stress can lead to a rise in the intracellular concentration of this metal. Also, MT expression following a hypoxic challenge is abolished in nonneuronal cell lines that are deficient in this promoter but not in their wild-type counterparts (Murphy et al., 1999). Furthermore, nitric oxide, an important mediator of cell death in many models of neurodegeneration (Aizenman et al., 1998), has been shown to mobilize intracellular zinc, most likely through its release from MT (Kroncke et al., 1994; Berendji et al., 1997; Cuajungco and Lees, 1998*b*; Aravindakumar et al., 1999; Pearce et al., 2000). Finally, peroxynitrite-induced cytotoxicity in isolated thymocytes was recently shown to be abolished by zinc chelation (Virag and Szabo, 1999).

Zn^{2+}-induced neurotoxicity exhibits features of both apoptosis and necrosis (E. Y. Kim et al., 1999; Y. H. Kim et al., 1999). In the present study we demonstrate that the putative Zn^{2+}-mediated DTDP toxicity likely involves the loss of intracellular potassium and is caspase-dependent, and it induces DNA laddering, all of which are associated with apoptotic processes. Although other studies have previously shown that there are increases in $[Zn^{2+}]_i$ in lymphocytes undergoing apoptosis (Zalewski et al., 1994), the mechanisms by which Zn^{2+} activates cell death pathways are not clear. Indeed, there are several reports suggesting that Zn^{2+} can also inhibit apoptosis (Zalewski et al., 1993; Perry et al., 1997; Chai et al., 1999; Ho et al., 2000), especially at high concentrations (Fraker and Telford, 1997). In those studies Zn^{2+} was shown to inhibit directly both caspase and endonuclease activity as well as prevent apoptosis due to Zn^{2+} deficiency induced by membrane-permeable chelators or dietary deprivation. These studies do not exclude the possibility that the impact of Zn^{2+} on cell viability is critically dependent on the intracellular Zn^{2+} concentration and subcellular localization, as has previously been suggested for Ca^{2+} in neural cells (Lipton and Kater, 1989; Gwag et al., 1999).

We show here that DTDP-induced cell death can be abrogated by high extracellular KCl levels and TEA, presumably be preventing the depletion of intracellular potassium. The efflux of this ion from cells has been implicated in neuronal apoptosis (Lee et al., 1999) and has been associated with activation of caspase-3 (Bortner et al., 1997). This enzyme, in turn, has been shown to activate selectively a caspase-dependent DNase, which causes the apoptotic fragmentation of DNA (Enari et al., 1998) and chromatin condensation (Sahara et al., 1999), both of which were observed in our studies. However, the mechanism by which Zn^{2+} may initiate this putative cascade process is not known.

Zn^{2+} may compromise energy production in neurons by depleting cellular levels of NAD and thereby inhibiting glycolysis (Sheline et al., 2000). Another possibility is that Zn^{2+} may mediate alterations in the function of the mitochondrion, an organelle that has been tightly linked to apoptosis on its dysfunction. In fact, Zn^{2+} has been suggested to inhibit the electron transport chain (Kleiner, 1974) and induce the production of mitochondrial-derived reactive oxygen species (Sensi et al., 1999). Therefore, inhibition of mitochondrial function and respiration may be a causative factor in Zn^{2+}-mediated DTDP toxicity (Brown et al., 2000). Consistent with this notion, Manev et al. (1997) previously associated mitochondrial dysfunction with neuronal Zn^{2+} toxicity. Zn^{2+} has also been shown to activate sphingomyelinase (Spence et al., 1989; Schissel et al., 1996), which leads to generation of ceramide, a known apoptogen (Hannun, 1994; Brugg et al., 1996), and can trigger the activation of mitogen-activated protein kinase pathways (Park and Koh, 1999). Zn^{2+} influx can induce expression of genes with MT promoters (Atar et al., 1995), and it is possible that oxidation-induced Zn^{2+} release from Zn^{2+}-containing DNA-binding proteins, including p53 (Fojta et al., 1999), might alter gene expression. Both of these effects could also contribute to DTDP-induced apoptotic cell death. In conclusion, our findings suggest that DTDP-induced Zn^{2+} release from intracellular stores can result in neuronal apoptosis. Given that oxidative stress is a common mechanism associated with cell death in several acute and chronic neurodegenerative conditions, we believe that oxidant-induced Zn^{2+} release may initiate a previously overlooked pathological cascade.

Acknowledgment: We thank D. Leszkiewicz, S. Du, and M. Tran for suggestions and help with some of the experiments and Dr. P. Land for many helpful discussions. This work was supported by grants NS29365 (to E.A.) and NS34138 (to I.J.R.) from the National Institutes of Health, a Grant-in Aid from the American Heart Association (to E.A.), grant 98292027 (to I.J.R.) from the USAMRMC, and the University of Pittsburgh Alzheimer's Disease Research Center (to B.A.M.). I.J.R. is an Established Investigator of the American Heart Association.

REFERENCES

Adler M., Shafer H., Hamilton T., and Petrali J. P. (1999) Cytotoxic actions of the heavy metal chelator TPEN on NG108–15 neuroblastoma–glioma cells. *Neurotoxicology* **20,** 571–582.

Ahn Y. H., Kim Y. H., Hong S. H., and Koh J. Y. (1998) Depletion of intracellular zinc induces protein synthesis-dependent neuronal apoptosis in mouse cortical culture. *Exp. Neurol.* **154,** 47–56.

Aizenman E., Hartnett K. A., and Reynolds I. J. (1990) Oxygen free radicals regulate NMDA receptor function via a redox modulatory site. *Neuron* **5,** 841–846.

Aizenman E., Brimecombe J. C., Potthoff W. K., and Rosenberg P. A. (1998) Why is the role of nitric oxide in NMDA receptor function and dysfunction so controversial? *Prog. Brain Res.* **118,** 53–71.

Andrews G. K. (1999) Regulation of metallothionein gene expression by oxidative stress and metal ions. *Biochem. Pharmacol.* **59,** 95–104.

Aniksztejn L., Charton G., and Ben-Ari Y. (1987) Selective release of endogenous zinc from the hippocampal mossy fibers in situ. *Brain Res.* **404,** 58–64.

Aravindakumar C. T., Ceulemans J., and DeLey M. (1999) Nitric oxide induces Zn^{2+} release from metallothionein by destroying zinc–sulfur clusters without concomitant formation of *S*-nitrosothiol. *Biochem. J.* **344,** 253–258.

Arslan P., Virgilio F. D., Beltrame M., Tsien R. Y., and Pozzan T. (1985) Cytosolic Ca^{2+} homeostasis in Ehrlich and Yoshida carcinomas. A new, membrane permeant chelator of heavy metals reveals that these ascites tumor cell lines have normal cytosolic free Ca^{2+}. *J. Biol. Chem.* **260,** 2719–2727.

Assaf S. Y. and Chung S. H. (1984) Release of endogenous Zn^{2+} from brain tissue during activity. *Nature* **308,** 734–736.

Atar D., Backx P. H., Appel M. M., Gao W. D., and Marban E. (1995) Excitation–transcription coupling mediated by zinc influx through voltage dependent calcium channels. *J. Biol. Chem.* **270,** 2473–2477.

Berg J. M. (1990) Zinc fingers and other metal-binding domains. Elements for interactions between macromolecules. *J. Biol. Chem.* **265,** 6513–6516.

Berendji D., Kolb-Bachofen V., Meyer K. L., Grapenthin O., Weber H., Wahn V., and Kroncke K. D. (1997) Nitric oxide mediates intracytoplasmic and intranuclear zinc release. *FEBS Lett.* **405,** 37–41.

Bortner C. D., Hughes F. M. J. Jr., and Cidlowsky J. A. A. (1997) A primary role for K^+ and Na^+ efflux in the activation of apoptosis. *J. Biol. Chem.* **272,** 32436–32442.

Brown A. M., Kristal B. S., Effron M. S., Shestopalov A. I., Ulucci P. A., Sheu K.-F. R., Blass J. P., and Cooper A. J. L. (2000) Zn^{2+}

inhibits α-ketoglutarate-stimulated mitochondrial respiration and the isolated α-ketoglutarate dehydrogenase complex. *J. Biol. Chem.* **275,** 13441–13447.

Brugg B., Michel P. P., Agid Y., and Ruberg M. (1996) Ceramide induces apoptosis in cultured mesencephalic neurons. *J. Neurochem.* **66,** 733–739.

Canzoniero L. M., Sensi S. L., and Choi D. W. (1997) Measurement of intracellular free zinc in living neurons. *Neurobiol. Dis.* **4,** 275–279.

Chai F., Truong-Tran A. Q., Ho L. H., and Zalewski P. D. (1999) Regulation of caspase activation and apoptosis by cellular zinc fluxes and zinc deprivation: a review. *Immunol. Cell. Biol.* **77,** 272–278.

Cheng C. and Reynolds I. J. (1998) Calcium-sensitive fluorescent dyes can report increases in intracellular free zinc concentration in cultured forebrain neurons. *J. Neurochem.* **71,** 2401–2410.

Choi D. W., Yokoyama M., and Koh J. (1988) Zinc neurotoxicity in cortical cell culture. *Neuroscience* **24,** 67–79.

Cornell N. W. and Crivaro K. E. (1972) Stability constant for the zinc–dithiothreitol complex. *Anal. Biochem.* **47,** 203–208.

Csermely P., Sandor P., Radics L., and Somogyi J. (1989) Zinc forms complexes with higher kinetical stability than calcium, 5-F-BAPTA as a good example. *Biochem. Biophys. Res. Commun.* **165,** 838–844.

Cuajungco M. P. and Lees G. J. (1998*a*) Diverse effects of metal chelating agents on the neuronal cytotoxicity of zinc in the hippocampus. *Brain Res.* **799,** 97–107.

Cuajungco M. P. and Lees G. J. (1998*b*) Nitric oxide generators produce accumulations of chelatable zinc in hippocampal neuronal perikarya. *Brain Res.* **799,** 118–129.

Dalton T. P., Li Q., Bittel D., Liang L., and Andrews G. K. (1996) Oxidative stress activates metal-responsive transcription factor-1 binding activity. Occupancy in vivo of metal response elements in the metallothionein-I gene promoter. *J. Biol. Chem.* **271,** 26233–26241.

Dineley K. E., Scanlon J. M., Kress G. J., Stout A. K., and Reynolds I. J. (2000) Astrocytes are more resistant than neurons to the cytotoxic effects of increased $[Zn^{2+}]_i$. *Neurobiol. Dis.* (in press).

Eager K. R., Roden L. D., and Dulhunty A. F. (1997) Actions of sulfhydryl reagents on single ryanodine receptor Ca^{2+}-release channels from sheep myocardium. *Am. J. Physiol.* **272,** C1908–C1918.

Enari M., Sakahira H., Yokoyama H., Okawa K., Iwamatsu A., and Nagata S. (1998) A caspase-dependent DNase that degrades DNA during apoptosis, and its inhibitor ICAD. *Nature* **391,** 43–50.

Fojta M., Kubicarova T., Vojtesek B., and Palecek E. (1999) Effect of p53 protein redox states on binding to supercoiled and linear DNA. *J. Biol. Chem.* **274,** 25749–25755.

Fraker P. J. and Telford W. G. (1997) A reappraisal of the role of zinc in life and death decisions of cells. *Proc. Soc. Exp. Biol. Med.* **215,** 229–236.

Frederickson C. J. (1989) Neurobiology of zinc and zinc-containing neurons. *Int. Rev. Neurobiol.* **31,** 145–238.

Frederickson C. J., Hernandez M. D., Goik S. A., Morton J. D., and McGinty J. F. (1988) Loss of zinc staining from hippocampal mossy fibers during kainic acid induced seizures: a histofluorescence study. *Brain Res.* **446,** 383–386.

Grynkiewicz G., Poenie M., and Tsien R. Y. (1985) A new generation of Ca^{2+} indicators with greatly improved fluorescence properties. *J. Biol. Chem.* **260,** 3440–3450.

Gwag B. J., Canzoniero L. M., Sensi S. L., Demaro J. A., Koh J. Y., Goldberg M. P., Jacquin M., and Choi D. W. (1999) Calcium ionophores can induce either apoptosis or necrosis in cultured cortical neurons. *Neuroscience* **90,** 1339–1348.

Hannun Y. A. (1994) The sphingomyelin cycle and the second messenger function of ceramide. *J. Biol. Chem.* **269,** 3125–3128.

Hartnett K. A., Stout A. K., Rajdev S., Rosenberg P. A., Reynolds I. J., and Aizenman E. (1997) NMDA receptor-mediated neurotoxicity: a paradoxical requirement for extracellular Mg^{2+} in Na^+/Ca^{2+}-free solutions in rat cortical neurons in vitro. *J. Neurochem.* **68,** 1836–1845.

Ho L. H., Ratnaike R. N., and Zalewski P. D. (2000) Involvement of intracellular labile zinc in suppression of DEVD-caspase activity in human neuroblastoma cells. *Biochem. Biophys. Res. Commun.* **268,** 148–154.

Howell G. A., Welch M. G., and Frederickson C. J. (1984) Stimulation-induced uptake and release of zinc in hippocampal slices. *Nature* **308,** 736–738.

Jacob C., Maret W., and Vallee B. L. (1998) Control of zinc transfer between thionein, metallothionein and zinc proteins. *Proc. Natl. Acad. Sci. USA* **95,** 3489–3494.

Jiang L. J., Maret W., and Vallee B. L. (1998) The glutathione redox couple modulates zinc transfer from metallothionein to zinc-depleted sorbitol dehydrogenase. *Proc. Natl. Acad. Sci. USA* **95,** 3483–3488.

Kim E. Y., Koh J. Y., Kim Y. H., Sohn S., Joe E., and Gwag B. J. (1999) Zn^{2+} entry produces oxidative neuronal necrosis in cortical cell cultures. *Eur. J. Neurosci.* **11,** 327–334.

Kim Y. H., Kim E. Y., Gwag B. J., Sohn S., and Koh J. Y. (1999) Zinc-induced cortical neuronal death with features of apoptosis and necrosis: mediation by free radicals. *Neuroscience* **89,** 175–182.

Kleiner D. (1974) The effect of Zn^{2+} ions on mitochondrial electron transport. *Arch. Biochem. Biophys.* **165,** 121–125.

Koh J.-Y. and Choi D. W. (1994) Zinc toxicity on cultured cortical neurons: involvement of *N*-methyl-D-aspartate receptors. *Neuroscience* **60,** 1049–1057.

Koh J.-Y., Suh S. W., Gwag B. J., He Y. Y., Hsu C. Y., and Choi D. W. (1996) The role of zinc in selective neuronal death after transient global cerebral ischemia. *Science* **272,** 1013–1016.

Kroncke K. D., Fehsel K., Schmidt T., Zenke F. T., Dasting I., Wesener J. R., Betterman H., Breunig K. D., and Kolb-Bachofen V. (1994) Nitric oxide destroys zinc–sulfur clusters inducing zinc release from metallothionein and inhibition of the zinc finger-type yeast transcription activator LAC9. *Biochem. Biophys. Res. Commun.* **200,** 1105–1110.

Lee J.-M., Zipfel G. J., and Choi D. W. (1999) The changing landscape of ischaemic brain injury mechanisms. *Nature* **399** (Suppl.), A7–A14.

Lee J.-Y., Park J., Kim Y.-H., Kim D. H., Kim C. G., and Koh J.-Y. (2000) Induction by synaptic zinc of heat shock protein-70 in hippocampus after kainate seizures. *Exp. Neurol.* **161,** 433–441.

Lipton S. A. and Kater S. B. (1989) Neurotransmitter regulation of neuronal outgrowth, plasticity and survival. *Trends Neurosci.* **12,** 265–270.

Manev H., Kharlamov E., Uz T., Mason R. P., and Cagnoli C. M. (1997) Characterization of zinc-induced neuronal death in primary cultures of rat cerebellar granule cells. *Exp. Neurol.* **146,** 171–178.

Maret W. and Vallee B. L. (1998) Thiolate ligands in metallothionein confer redox activity on zinc clusters. *Proc. Natl. Acad. Sci. USA* **95,** 3478–3482.

McLaughlin B. A., Nelson D., Silver I. A., Erecińska M., and Chesselet M. F. (1998) Methylmalonate toxicity in primary neuronal cultures. *Neuroscience* **86,** 279–290.

Murphy B. J., Andrews G. K., Bittel D., Discher D. J., McCue J., Green C. J., Yanovsky M., Giaccia A., Sutherland R. M., Laderoute K. R., and Webster K. A. (1999) Activation of metallothionein gene expression by hypoxia involves metal response elements and metal transcription factor-1. *Cancer Res.* **59,** 1315–1322.

Park J. A. and Koh J. Y. (1999) Induction of an immediate early gene egr-1 by zinc through extracellular signal-regulated kinase activation in cortical culture: its role in zinc-induced neuronal death. *J. Neurochem.* **73,** 450–456.

Pearce L. L., Gandley R. E., Han W., Wasserloos K., Stitt M., Kanai A. J., McLaughlin M. K., Pitt B. R., and Levitan E. S. (2000) Role of metallothionein in nitric oxide signaling as revealed by a green fluorescent fusion protein. *Proc. Natl. Acad. Sci. USA* **97,** 477–482.

Perry D. K., Smyth M. J., Stennicke H. R., Salvesen G. S., Duriez P., Poirier G. G., and Hannun Y. A. (1997) Zinc is a potent inhibitor of the apoptotic protease, caspase-3. A novel target for zinc in the inhibition of apoptosis. *J. Biol. Chem.* **272,** 18530–18533.

Rosenberg P. A. (1991) Accumulation of extracellular glutamate and neuronal death in astrocyte-poor cortical cultures exposed to glutamine. *Glia* **4,** 91–100.

Rosenberg P. A. and Aizenman E. (1989) Hundred-fold increase in neuronal vulnerability to glutamate toxicity in astrocyte-poor cultures of rat cerebral cortex. *Neurosci. Lett.* **103,** 162–168.

Sahara S., Aoto M., Eguchi Y., Imamoto N., Yoneda Y., and Tsujimoto Y. (1999) Acinus is a caspase-3-activated protein required for apoptotic chromatin condensation. *Nature* **401,** 168–173.

Schissel S. L., Schuchman E. H., Williams K. J., and Tabas I. (1996) Zn^{2+}-stimulated sphingomyelinase is secreted by many cell types and is a product of the acid sphingomyelinase gene. *J. Biol. Chem.* **271,** 18431–18436.

Sensi S. L., Canzoniero L. M., Yu S. P., Ying H. S., Koh J. Y., Kerchner G. A., and Choi D. W. (1997) Measurement of intracellular free zinc in living cortical neurons: routes of entry. *J. Neurosci.* **17,** 9554–9564.

Sensi S. L., Yin H. Z., Carriedo S. G., Rao S. S., and Weiss J. H. (1999) Preferential Zn^{2+} influx through Ca^{2+}-permeable AMPA/kainate channels triggers prolonged mitochondrial superoxide production. *Proc. Natl. Acad. Sci. USA* **96,** 2414–2419.

Sheline C. T., Behrens M. M., and Choi D. W. (2000) Zinc-induced cortical neuronal death: contribution of energy failure attributable to loss of NAD^+ and inhibition of glycolysis. *J. Neurosci.* **20,** 3139–3146.

Shumaker D. K., Vann L. R., Goldberg M. W., Allen T. D., and Wilson K. L. (1998) TPEN, a Zn^{2+}/Fe^{2+} chelator with low affinity for Ca^{2+}, inhibits lamin assembly, destabilizes nuclear architecture and may independently protect nuclei from apoptosis in vitro. *Cell Calcium* **23,** 151–164.

Simons T. J. B. (1993) Measurement of free Zn^{2+} ion concentration with the fluorescent probe mag-fura-2 (furaptra). *J. Biochem. Biophys. Methods* **27,** 25–37.

Sloviter R. S. (1985) A selective loss of hippocampal mossy fiber Timm stain accompanies granule cell seizure activity induced by perforant path stimulation. *Brain Res.* **330,** 150–153.

Spence M. W., Byers D. M., Palmer F. B., and Cook H. W. (1989) A new Zn^{2+}-stimulated sphingomyelinase in fetal bovine serum. *J. Biol. Chem.* **264,** 5358–5363.

Stout A. K. and Reynolds I. J. (1999) High-affinity calcium indicators underestimate increases in intracellular calcium concentrations associated with excitotoxic glutamate stimulations. *Neuroscience* **89,** 91–100.

Virag L. and Szabo C. (1999) Inhibition of poly(ADP-ribose) synthetase (PARS) and protection against peroxynitrite-induced cytotoxicity by zinc chelation. *Br. J. Pharmacol.* **126,** 769–777.

Vogt K., Mellor J., Tong G., and Nicoll R. (2000) The actions of synaptically released zinc at hippocampal mossy fibers. *J. Neurosci.* **26,** 187–196.

Weiss J. H., Hartley D. M., Koh J.-Y., and Choi D. W. (1993) AMPA receptor activation potentiates zinc neurotoxicity. *Neuron* **10,** 43–49.

Yu S. P., Yeh C. H., Sensi S., Gwag B. J., Canzoniero L. M., Farhangrazi Z. S., Ying H. S., Tian M., Dugan L. L., and Choi D. W. (1997) Mediation of neuronal apoptosis by enhancement of outward potassium current. *Science* **278,** 114–117.

Zalewski P. D., Forbes I. J., and Betts W. H. (1993) Correlation of apoptosis with change in intracellular labile Zn(II) using zinquin [(2-methyl-8-*p*-toluenesulphonamido-6-quinolyloxy)acetic acid], a new specific fluorescent probe for Zn(II). *Biochem. J.* **296,** 403–408.

Zalewski P. D., Forbes I. J., Seamark R. F., Borlinghaus R., Betts W. H., Lincoln S. F., and Ward A. D. (1994) Flux of intracellular labile zinc during apoptosis (gene-directed cell death) revealed by a specific chemical probe, Zinquin. *Chem. Biol.* **1,** 153–161.